Oxide Multilayers

Saban M. HUS*
shus@utk.edu
The University of Tennessee Department of Physics and Astronomy,
Knoxville, TN 37922
Course: Solid State II (Spring 2008)
Instructor: Elbio Dagotto
(Dated: February 25, 2008)

The most common production techniques of oxide-multilayer structures has been summarized. Recently observed novel properties of oxide interfaces has been cited.

INTRODUCTION

Multilayer thin films have been attracting attention for half-century due to many possible applications ranging from protective coating to Laser Diodes. State of the art production techniques, made it possible to deposit high-quality multilayered thin films with atomically precise interfaces between different materials, including complex oxides with large and complicated unit cells [1].

Despite the better known properties of semiconductor-oxide multilayer films this paper will focus on the complex oxides which promise novel properties not achievable with ordinary semiconductors [1] [2]. Strongly correlated electron materials have very less common points compared the semiconductors. Therefore, properties of the multilayer structures built with these materials cannot be examined in a common basis. In the first section of this paper the most important production techniques which are used to deposit high quality thin films will be summarized. In the second part some of the novel properties observed in different oxide-multilayers will be cited.

DEPOSITION TECHNIQUES

Molecular Beam Epitaxy

Molecular beam epitaxy (MBE) was developed in the early 1970s as a means of growing high-purity epitaxial layers of compound semiconductors [3]. Since that time it has evolved into a popular technique for growing III-V compound semiconductors as well as several other materials. MBE can produce high-quality layers with very abrupt interfaces and good control of thickness, doping, and composition. Because of the high degree of control possible with MBE, it is a valuable tool in the development of sophisticated electronic and optoelectronic devices.

In MBE, the constituent elements of a semiconductor in the form of 'molecular beams' are deposited onto a heated crystalline substrate to form thin epitaxial layers. The 'molecular beams' are typically from thermally evaporated elemental sources, but other sources include metal-organic group III precursors (MOMBE), gaseous group V hydride or organic precursors (gas-source MBE), or some combination (chemical beam epitaxy or CBE). To obtain high-purity layers, it is critical that the material sources be extremely pure and that the entire process be done in an ultra-high vacuum (10^{-8} Pa) environment. Another important feature is that growth rates are typically on the order of a few $\AA$/s and the beams can be shuttered in a fraction of a second, allowing for nearly atomically abrupt transitions from one material to another. Fig. 1.

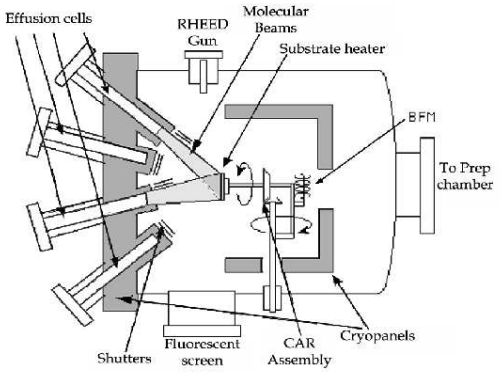

FIG. 1: Schematic view of a MBE system

Pulsed Laser Deposition

Pulsed-laser deposition (PLD) was the first technique used to successfully deposit a superconducting YBa2Cu3O7 thin films [4]. Since that time, many materials that are normally difficult to deposit by other methods, especially multi-element oxides, have been successfully deposited by PLD. As a result, PLD has gained a great deal of attention in the past few years for its ease of use and success in depositing materials of complex stoichiometry [5].

The main advantage of PLD derives from its laser material removal mechanism; PLD relies on a photon interaction to create an ejected plume of material from any

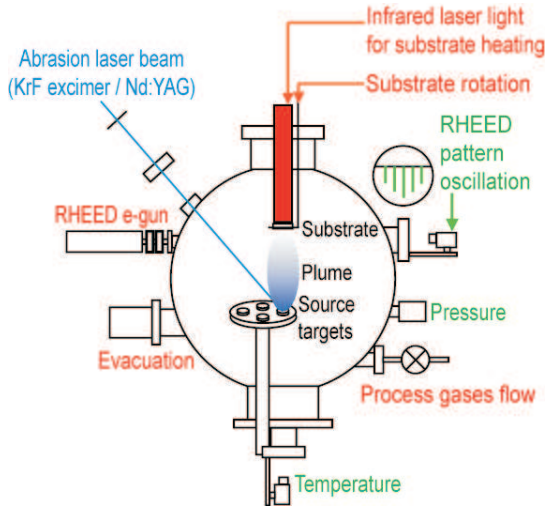

FIG. 2: Schematic view of an advanced PLD System developed by Pascal co. ltd (Japan)

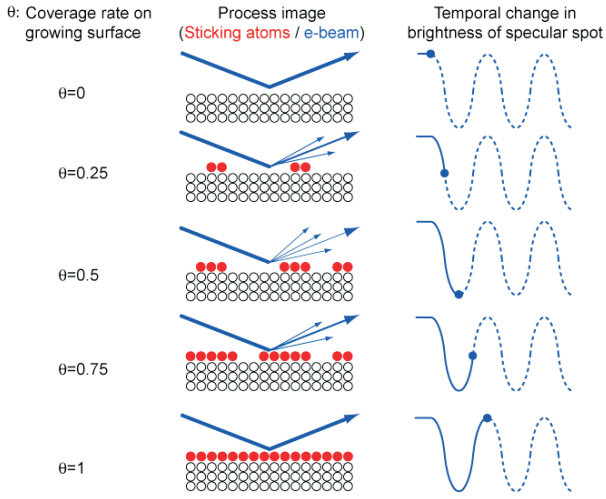

FIG. 3: Elastic scattering model of RHEED intensity oscillation in2-dim epitaxial growth

target. The laser-induced expulsion produces a plume of material with stoichiometry similar to the target. The vapor (plume) is collected on a substrate placed a short distance from the target. Though the actual physical processes of material removal are quite complex, one can consider the ejection of material to occur due to rapid explosion of the target surface due to superheating. Schematic view of an advanced PLD system is given in Fig. 2.

It is generally easier to obtain the desired film stoichiometry for multi-element materials using PLD than with other deposition technologies. Thermal evaporation technique which is used in MBE produces a vapor composition dependent on the vapor pressures of elements in the source material. In thermal evaporation the temperature of the source materials must be kept almost contant ($\pm 0.1\%$). This can be very difficult while evaporating oxides with melting points over 1000 K. An other important advantage of the PLD is its much faster deposition rates compared to MBE. Furthermore, it provides a better control on deposition rate and the film thickness because these parameters can be changed by changing the repetition rate of the laser pulse.

Reflection High-Energy Electron Diffraction

Reflection High-Energy Electron Diffraction (RHEED) is a versatile analytical tool for characterizing thin films during growth by MBE or PLD, since it is very sensitive to surface structure and morphology. RHEED is based on the reflection of electrons with high kinetic energy (typically in the 5-100 keV regime) and low impact angle (typically less than 5^o) from the surface of a solid. These scattered electron beam hit a fluorescent screen and forms a characteristic RHEED pattern depend on the morphology and roughness of the sample surface. Patterns are used to determine the crystal structure and constants of the sample. RHEED intensity depends on the film roughness, the growth process leads to intensity oscillations of the RHEED spots where a single oscillation usually corresponding to the completion of a single monolayer.Fig. 3 illustrates the RHEED intensity oscillations in2-dim epitaxial growth.

RECENT STUDIES ON OXIDE MULTILAYER STRUCTURES

An Enormous number of strongly correlated oxides have been synthesized as bulk materials and thin films. Many anomalous properties has been observed experimentally in these materials and different theoretical approaches has been developed [6]. The broad spectrum of intrinsic properties, including ferro-electricity and superconductivity, of these oxides can be combined to achieve physical properties that are not found in either of their constituents [7]. Only a few of the possible combinations of these oxides has been investigated but they have already showed interesting features such as high mobility [7][5] or superconductivity [8] at the interface, optical magnetoelectric effect [9].

Perovskite Oxides

Ohtomo et al. grew $SrTiO_3/LaTiO_3$ and $LaAlO_3/SrTiO_3$ superlattice films by laser pulsed deposition in an ultrahigh-vacuum chamber [10][7]. Both $LaAlO_3$ and $SrTiO_3$ are wide bandgap insulaters ($LaAlO_3$ ~5.6 eV, $SrTiO_3$ ~3.2 eV) and has close

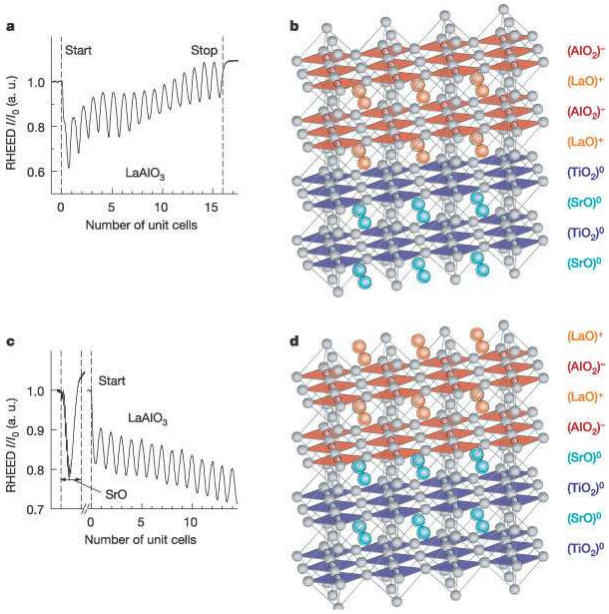

FIG. 4: **a:**, RHEED intensity oscillations of the specular reflected beam for the growth of LaAlO3 directly on the TiO2 terminated SrTiO3 (001) surface. **b:**, Schematic of the resulting (LaO)+/(TiO2)0 interface, showing the composition of each layer and the ionic charge state of each layer. **c:**, RHEED oscillations for the growth of LaAlO3, after a monolayer of SrO was deposited on the TiO2 surface. **d:**, Schematic of the resulting (AlO2)-/(SrO)0 interface.

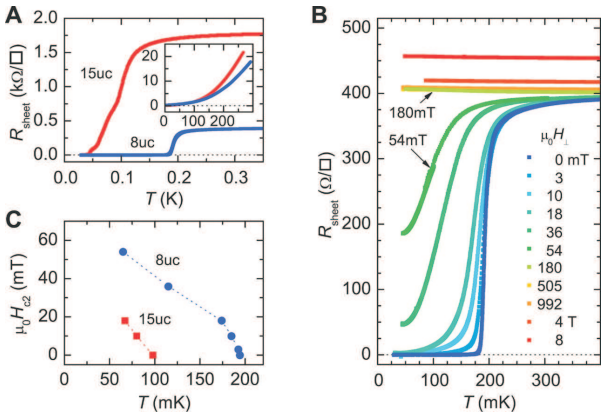

FIG. 5: Transport measurements on $LaAlO_3/SrTiO_3$ heterostructures. **a:**, Dependence of the sheet resistance on T of the 8-uc and 15-uc samples (measured with a 100-nA bias current). (Inset) Sheet resistance versus temperature measured between 4 K and 300 K. **b:** Sheet resistance of the 8-uc sample plotted as a function of T for magnetic fields applied perpendicular to the interface. **c:** Temperature dependence of the upper critical field H_{c2} of the two samples.

lattice constants ($LaAlO_3$ ~3.789Å, $SrTiO_3$ ~3.905Å, $LaTiO_3$ ~3.97Å). Schematic models of two possible interfaces between $LaAlO_3$ and $SrTiO_3$ in the (001) orientation has been given in Fig. 4. The presence of dangling bonds and incomplete atomic coordinations leads to a nontrivial electronic structure at the interface between these crystalline materials. The formal valance states can be assigned as La^{3+}, Al^{3+}, O^{2-}, Sr^{2+} and Ti^{4+}. To first order, only Ti has an accessible mixed valance character and can reduce towards Ti^{3+}. In this structure $SrTiO_3$ is a sequence of charge neutral sheets, Whereas $LaAlO_3$ alternates between $\pm e$ charged sheets. In the simple ionic limit, the interface presents an extra half electron or hole per two dimensional unit cell. Conductivity and Hall coefficient of the interface was measured with the help of the laser annealed ohmic contacts which can reach the buried interface. The hole-doped interface is found to be insulating while the electron-doped interface has a very high carrier mobility exceeding 10,000 $cm^2V^{-1}s^{-1}$. Also dramatic magnetoresistance oscillations periodic with the inverse magnetic field have been observed at low temperatures.

Later, Thiel et al. [11] reported a large electric-field response of quasi-two dimensional electron gases generated at the interfaces between LaAlO3 and SrTiO3. They have been able to modulate the conductivity of the electron gas by applying a gate voltage. These device presents an oxide analog of semiconducting high electron mobility transistors. Finally Reyren et al. [8] reported superconductivity in this electron gas with a transition temperature of 200mK (Fig. 5).

$SrTiO_3/LaTiO_3$ superlattices grown by Ohtomo et al.[10] have been used to examine the microscopic electronic structure of the complex oxides. Using an atomic scale electron beam they have observed that the spatial distribution of the extra electron in the titanium sites results in metallic conductivity in the interface. In this work it has been showed that the electron gas is confined within a ~ 2-nm thick layer. Their capability of depositing atomically abrupt layers of $LaTiO_3$ (Fig. 6) has allowed them to understand the transition from the bulk like to short-scale electronic properties. Theoretical analysis of these structures has also been widely studied [12]. In a different study Yamada et al. [13] showed that a $LaAlO_3/La_{0.6}Sr_{0.4}MnO_3/SrTiO_3$ superlattice exhibits very large magnetization induced second harmonic generation. They have also showed that by grading the doping profile on an atomic scale at the interface, a robust ferro-magnetism can be realized around room temperature. These results may lead to high performance spin tunnel junctions.

The magnetoelectric effect is induction of polarization by a magnetic field or induction of magnetization by an electric field [14]. Recently, magnetoelectric effect at optical frequencies has been observed in superlattices composed of LaMnO3, SrMnO3, and LaAlO3 [9].

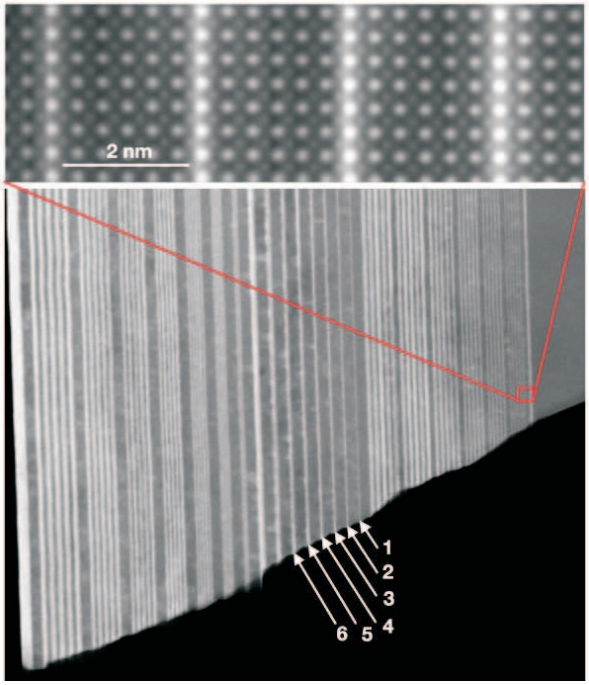

FIG. 6: The view is down the [100] zone axis of the SrTiO3 substrate, which is on the right. After depositing initial calibration layers, the growth sequence is 5 n (that is, 5 layers of SrTiO3 and n layers of LaTiO3), 20 n, n n, and finally a LaTiO3 capping layer. The numbers in the image indicate the number of LaTiO3 unit cells in each layer. Field of view, 400 nm. Top, a magnified view of the 5 1 series. The raw images have been convolved with a 0.05-nm-wide gaussian to reduce noise.

Superconductor-Ferroelectric Multilayers

High transition-temperature superconductivity is the most exotic property observed in complex oxides. Superconductor-Ferromagnetic multilayers may also lead to new novel properties. High quality multilayers of La0.67Sr0.33MnO3/ YBa2Cu3O7 has been deposited by sputtering in order to better understand the transport and magnetic properties of these materials [15].

In a recent study with the same materials it has been observed that a charge transfer from Mg to Cu ions occurs across the interface. This induces important modifications in the valance electron clouds around these atoms and forms a strong chemical bond between Cu and Mg atoms across the interface [1].

In order to study the behavior of electrons at the buried interfaces Chakhalian et al. used x-rays with tunable energy and polarization from a synchrotron source. Energy of the x-ray photons has been tuned to observe absorption peaks corresponding to intra-ionic transition $2p^6 3d^9 \rightarrow 2p^5 3d^{10}$ (913eV)at Cu L_3 absorption edge. Using beams with polarizations parallel or perpendicular to the interface, they obtained information about the difference between shape of the valance-electron clouds of the Mg and Cu atoms at the interface and bulk. They have observed a shift (∼0.4eV)in the absorbtion peak. This shift is evidence of a change in valance state of Cu ions near the interface. They have concluded that some of the holes which are constrained to the Cu $d_{x^2-y^2}$ orbital in the bulk, occupy the $d_{3z^2-r^2}$ orbital at the interface. This process is called "orbital reconstruction".

* Electronic address: shus@utk.edu

[1] J. Chakhalian, J. W. Freeland, H. U. Habermeier, G. Cristiani, G. Khaliulin, , M. van Veenendaal, and B. Keimer, Science **318**, 1114 (2007).

[2] E. Dagotto, Science **318**, 1076 (2007).

[3] L. Businaro, *Fabrication and Characterization of Photonic Band Gap Materials* (Electronic Book, http://www.elettra.trieste.it/experiments/beamlines/lilit /htdocs/people/luca/tesihtml/tesimain.html, 2002), feb,19 2008.

[4] D. Dijkkamp and T. Venkatesan, Appl. Phys. Lett. **51** (1987).

[5] P. R. Willmott and J. B. Huber, Rev. Mod. Phys. **72** (2000).

[6] M. Imada, A. Fujimori, and Y. Tokura, Rev. Mod. Phys. **70**, 1039 (1998).

[7] A. Ohtomo and H. Y. Hwang, Nature **427**, 423 (2004).

[8] N. Reyren, S. Thiel, A. D. Caviglia, L. F. Kourkoutis, G. Hammerl, C. Richter, C. W. Schneider, T. Kopp, A.-S. Ruetschi, D. Jaccard, et al., Science **317**, 1196 (2007).

[9] N. Kida, H. Yamada, H. Sato, T. Arima, M. Kawasaji, H. Akoh, and Y. Tokura, Phys. Rev. Lett. **99**, 197404 (2007).

[10] A. Ohtomo, D. A. Muller, J. L. Grazul, and H. Y. Hwang, Nature **419**, 378 (2002).

[11] S. Thiel, G. Hammerl, A. Schmehl, C. W. Schneider, and J. Mannhart, Science **313**, 1942 (2006).

[12] S. Okomato, A. J. Millis, and N. A. Spaldin, Phys. Rev. Lett. **97**, 056802 (2006).

[13] H. Yamada, Y. Ogawa, Y. Ishii, H. Sato, M. Kawasaki, H. Akoh, and Y. Tokura, Science **305**, 646 (2004).

[14] Y. Tokura, Science **312** (2006).

[15] P. Przyslupski, I. Komissarov, W. Paszkowicz, P. Dluzewski, R. Minikayev, and M. Sawicki, Phys. Rev. B **69**, 134428 (2004).